ACS Energy LETTERS

Cite This: ACS Energy Lett. 2019, 4, 375−376

http://pubs.acs.org/journal/aelccp

ENERGY EXPRESS

Formation of Magnesium Dendrites during Electrodeposition

Rachel Davidson,[†,‡] Ankit Verma,[§] David Santos,[†,‡] Feng Hao,[§] Coleman Fincher,[⊥] Sisi Xiang,[‡] Jonathan Van Buskirk,[†,‡] Kelvin Xie,[‡] Matt Pharr,[⊥] Partha P. Mukherjee,*[,§] and Sarbajit Banerjee*[,†,‡]

[†]Department of Chemistry, [‡]Department of Materials Science & Engineering, and [⊥]Department of Mechanical Engineering, Texas A&M University, College Station, Texas 77843, United States

[§]School of Mechanical Engineering, Purdue University, West Lafayette, Indiana 47907, United States

Supporting Information

ABSTRACT: We demonstrate the growth of dendritic magnesium deposits with fractal morphologies exhibiting shear moduli in excess of values for polymeric separators upon the galvanostatic electrodeposition of metallic Mg from Grignard reagents in symmetric Mg−Mg cells. Dendritic growth is understood on the basis of the competing influences of reaction rate, electrolyte transport rate, and self-diffusion barrier.

The use of lithium-ion batteries (LIBs) as a means of energy storage is pervasive across most types of consumer electronics and is on the ascent for large-area formats such as electric vehicles. Current commercial LIBs pair transition-metal oxide cathodes with graphite anodes. A substantial enhancement of performance metrics is conceptually possible through the use of lithium metal anodes.[1] However, Li metal has a high propensity for dendrite formation.[2]

Magnesium batteries have attracted considerable attention as a potential alternative to lithium owing to the divalent nature of Mg ions, which can result in higher energy densities. The higher crustal abundance of magnesium as compared to lithium, its resilience to criticality constraints, and the apparent "non-dendrite" forming nature of this metal upon electroplating has focused considerable attention on this alternative energy storage vector.[3−9] Despite considerable focus on electrolyte development, the intrinsic electrodeposition process remains relatively scarcely explored.[10−13] The idea of a lower propensity toward dendrite formation has been uncritically accepted across a vast swath of the literature, even though most studies are limited in their exploration of deposition conditions. In this work, we demonstrate the electrochemical growth of fractal Mg dendrites from Grignard reagents in symmetric cells under galvanostatic conditions as described in the Supporting Information.

Figure S1 shows SEM images of the surfaces of Mg ribbon electrodes attesting to their smooth initial topographies. Videos S1−S3 illustrate time-lapse images (4000× speed) of Mg deposition monitored in situ with applied current densities of 0.307, 0.921, and 1.54 mA/cm^2 and average measured overpotentials of 0.278, 0.432, 0.668 V/mm, respectively, from a 0.5 M MeMgCl solution in THF over 8 h. Figure 1A shows

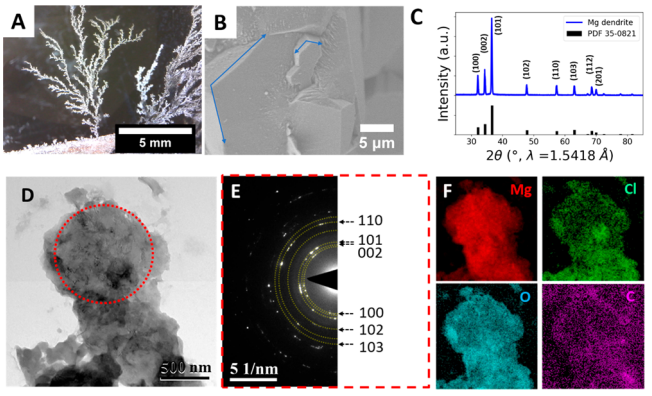

Figure 1. Characterization of Fractal Mg deposits: (A) Digital photograph of fractal Mg structure; (B) SEM image of a section of the structure; (C) powder XRD pattern measured for detached Mg fractal deposit; (D) TEM image of a region of polycrystalline Mg dendrites; (E) SAED pattern acquired from the region delineated by the red circle; (F) EDS maps of the region imaged in panel D.

images of fractal deposits formed from the electrodeposition of Mg from a 0.5 M solution of MeMgCl in THF at a constant current density of 0.921 mA/cm^2. Video S4 shows a tomographic reconstruction of a dendrite. SEM images indicate aggregated hexagonal platelets that are crystallized in the intrinsic habit of hcp Mg (angles of 118−121° between adjacent faces as shown in Figure 1B). A powder XRD pattern of the deposits can be indexed to PDF 35-0821, corresponding to hcp magnesium. Figure 1D shows a representative transmission

Received: December 17, 2018
Accepted: December 26, 2018
Published: December 26, 2018

DOI: 10.1021/acsenergylett.8b02470
ACS Energy Lett. 2019, 4, 375−376

electron microscopy (TEM) image. A selected area electron diffraction (SAED) pattern (Figure 1E) shows diffraction spots indicative of a well-developed polycrystalline structure. Energy dispersive spectroscopy (EDS) mapping indicated that the Mg dendrite is rich in Mg with trace amounts of Cl (Figure 1F). On the basis of 12 nanoindentation measurements, dendritic Mg exhibits an elastic modulus of 27.1 ± 2.8 GPa (Figure S2 A,B). Additionally, representative hardness versus depth and elastic modulus versus depth curves are shown in Figure S2. Following the Newman and Monroe criterion,[14] this translates to the need for a separator or solid-state electrolyte with a shear modulus of greater than ca. 24 GPa, indicating that Mg dendrites will readily puncture commonly used polymeric separators. Indeed, this value is much greater than the estimated 6.8 GPa reported for lithium deposits.[14] Notably, in "beyond-Li" chemistries, the metals typically have substantially greater elastic moduli than lithium, thereby posing a greater risk of rupturing separators upon dendrite formation.

To examine the balance between the surface diffusion and the electrochemical reaction rate, a nondimensional electrochemical Damköhler number, *Da*, can be defined as the ratio of the electrochemical reaction rate, k_e, to the surface diffusion rate, k_d, as[15]

$$Da = \frac{k_e}{k_d} \tag{1}$$

Values of $Da \gg 1$ imply that the electrochemical reaction occurs at a much faster rate as compared to surface self-diffusion (see the Supporting Information). In this limit, dendritic structures are expected, as observed in Figure 1, because despite the low calculated surface diffusion barriers for Mg,[6] the large monomer flux shifts the system to a reaction-dominated growth regime.[6,15] Figure 2A plots the different regimes in terms of the predicted

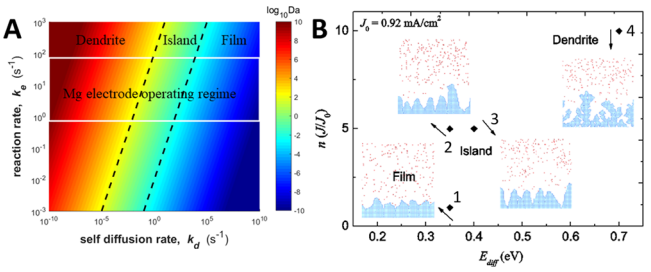

Figure 2. (A) Predicted deposition morphology phase plotted as a function of Damköhler number. (B) Deposition morphology predicted by KMC simulations for different values of current density and diffusion barriers.

morphologies of electroplated Mg deposits as a function of the electrochemical reaction and surface diffusion rates. The operating regime is delineated by white lines based on electrochemical reaction and surface diffusion rates noted in Tables S1 and S2.

Figure 2B shows the deposition morphologies obtained from mesoscale kinetic Monte Carlo (KMC) simulations upon varying the current density and self-diffusion activation barrier. Under conditions of high current densities and high self-diffusion energy barriers (top-right of Figure 2B), a strong propensity to form dendritic structures is clearly observed (marker 4 corresponds to J = 9.2 mA/cm^2, E_{diff} = 0.7 eV).

Strong electric fields (and consequently electrolyte potential gradients) occur at locations along the surface where the electrode is most curved. Consequently, the corners provide preferential deposition sites. This phenomenon is also observed at dendrite tips and electrode surface protrusions.[16]

Galvanostatic electrodeposition of metallic Mg from Grignard reagents in symmetric Mg−Mg cells demonstrates growth of highly anisotropic fractal deposits that are predominantly zerovalent magnesium. While the generalizability of the observed phenomena to other electrolytes and full cells remains to be established, it is worth noting that electrochemical reaction rates can quite readily surpass self-diffusion rates as a result of local inhomogeneities and reactivity. Lower operational temperatures, localization of overpotential at the anode edges, and fast charge rates will likely further exacerbate dendritic growth. The possibility for formation of "dead magnesium" caused by stripping at the base from high-aspect-ratio structures during discharge will require future consideration.[2] Though considerable effort has been invested in the development of Mg and other "beyond-Li" chemistries, further study is clearly required and the term "dendrite-free" must be used with caution.

■ ASSOCIATED CONTENT

Supporting Information

The Supporting Information is available free of charge on the ACS Publications website at DOI: 10.1021/acsenergylett.8b02470.

SEM images, data tables, and figures (PDF)
Video S1 (see text for description) (AVI)
Video S2 (see text for description) (AVI)
Video S3 (see text for description) (AVI)
Video S4 (see text for description) (AVI)

■ AUTHOR INFORMATION

Corresponding Authors

*E-mail: banerjee@chem.tamu.edu.
*E-mail: pmukherjee@purdue.edu.

ORCID

Sarbajit Banerjee: 0000-0002-2028-4675

Notes

The authors declare no competing financial interest.

■ ACKNOWLEDGMENTS

C.F. acknowledges NSF 1746932. This work was supported by the NSF under DMR 1809866 and 1805656.

■ REFERENCES

(1) Liu, B.; et al. *Joule* **2018**, *2* (5), 833−845.
(2) Chen, K.-H.; et al. *J. Mater. Chem. A* **2017**, *5* (23), 11671−11681.
(3) Aurbach, D.; et al. *Electrochem. Solid-State Lett.* **2001**, *4* (8), A113.
(4) Muldoon, J.; et al. *Energy Environ. Sci.* **2012**, *5* (3), 5941.
(5) Yoo, H. D.; et al. *Energy Environ. Sci.* **2013**, *6* (8), 2265−2279.
(6) Jäckle, M.; et al. *Energy Environ. Sci.* **2018**, *11* (12), 3400−3407.
(7) Canepa, P.; et al. *Chem. Rev.* **2017**, *117* (5), 4287−4341.
(8) Andrews, J. L.; et al. *Chem.* **2018**, *4* (3), 564−585.
(9) De Jesus, L. R.; et al. *ACS Energy Lett.* **2018**, *3*, 915.
(10) DeWitt, S.; et al. *J. Electrochem. Soc.* **2016**, *163* (3), A513−A521.
(11) Matsui, M.; et al. *J. Power Sources* **2011**, *196* (16), 7048−7055.
(12) Ling, C.; et al. *Electrochim. Acta* **2012**, *76*, 270−274.
(13) Jäckle, M.; et al. *J. Chem. Phys.* **2014**, *141*, 174710.
(14) Monroe, C.; et al. *J. Electrochem. Soc.* **2005**, *152* (2), A396−A404.
(15) Hao, F.; et al. *ACS Appl. Mater. Interfaces* **2018**, *10* (31), 26320.
(16) Akolkar, R.; et al. *J. Power Sources* **2013**, *232*, 23−28.

DOI: 10.1021/acsenergylett.8b02470
ACS Energy Lett. 2019, 4, 375−376